Research Report

98-14

Complex Vector Model of the Squirrel Cage Induction Machine Including Instantaneous Rotor Bar Currents

A. Munoz-Garcia, T.A. Lipo

Wisconsin Power Electronic Research Center
University of Wisconsin-Madison
Madison WI 53706-1691

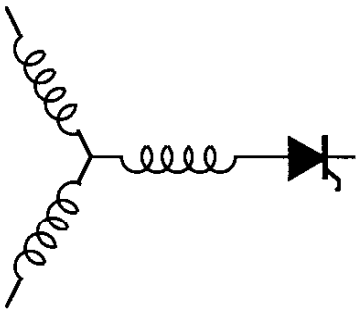

Wisconsin
Electric
Machines &
Power
Electronics
Consortium

University of Wisconsin-Madison
College of Engineering
Wisconsin Power Electronics Research Center
2559D Engineering Hall
1415 Engineering Drive
Madison WI 53706-1691

COMPLEX VECTOR MODEL OF THE SQUIRREL CAGE INDUCTION MACHINE INCLUDING INSTANTANEOUS ROTOR BAR CURRENTS

Alfredo Muñoz-García Thomas A. Lipo
Department of Electrical and Computer Engineering
University of Wisconsin - Madison
1415 Engineering Drive
Madison, WI 53706-1691 USA
Tel.: (608) 262-0727 Fax: (608) 262-1267 email: alfredo@cae.wisc.edu - lipo@engr.wisc.edu

Abstract—**In this paper a new detailed mathematical derivation of the squirrel cage induction machine d-q model is introduced. The model is based on coupled magnetic circuit theory and complex space vector notation and takes into account the actual non-sinusoidal rotor bar distribution. It is shown for the first time that, given the structural symmetry of the induction machine, both stator and rotor circuits can be modeled by the simple set of only four coupled differential equations. More important, the number of equations does not depend on the number of rotor bars and the model is valid even if the number of bars per pole is not an integer number. This enormous simplification is achieved without loss of generality nor loss of any information contained in the full set of equations and it is valid for any operating condition. The actual n rotor bars and end-ring currents are fully included in the model and they are obtained directly by using a simple vector transformation. In addition, the three-phase rotor equivalent parameters are obtained. Second order effects, such as skin effect in the rotor bars, can be taken into account by simply modifying the bar and end ring resistance values. An equivalent circuit based on the model is also derived.**

Since the number of equations needed is only four (the same as in the equivalent dq model) the computation effort required to solve the full system is drastically reduced.

I. Introduction

The well known dq model of induction machines is based on the assumption that both stator and rotor windings are sinusoidally distributed in space. Although the rotor cage is clearly non-sinusoidally distributed it is claimed that it can be replaced by an equivalent distributed winding [1], [2], [3]. A formal derivation of such an equivalence however is rarely found in the literature and in those few cases where a more formal approach has been adopted the derivation becomes very complex requiring simplifying assumptions [4], [5].

In the past several authors have used the coupled magnetic circuit theory to model a squirrel cage induction machine [6], [7], [9], [10], [13]. In general, for a machine having n rotor bars this approach leads to a model having n+3 non-linear simultaneous differential equations (plus the mechanical equation) requiring huge computational power [6], [7]. Although the number of equations can be somewhat reduced when there is an integer number of rotor bars per pole, the task of solving such a system of differential equations remains a formidable one.

In this paper it is shown that by using a particular space vector transformation the machine can be fully modeled using only four coupled differential equations. This enormous simplification is achieved without loss of generality nor loss of any information contained in the full set of equations and it is valid for any operating condition. More important, the number of equations does not depend on the number of rotor bars and it is valid even if the number of bars per pole is not an integer number. The model predicts the three-phase rotor equivalent parameters in terms of the actual rotor bar resistance and inductance values as well as giving the actual rotor bar and end-ring currents. Since the model uses the actual rotor bar and end-ring parameters, second order effects such as skin effect, can be easily incorporated.

II. Stator Model

The coupled magnetic circuit theory and complex space vector representation will be used through out the derivation. This technique is chosen because of the great deal of simplification that can be achieved as well as its generality. The following general assumptions are made:

- negligible saturation,
- uniform air-gap,
- stator windings sinusoidally distributed, *and*
- negligible inter-bar current

Although a sinusoidally distributed stator winding is assumed other winding distributions could also be analyzed by simply using superposition. This approach is justified by the well known fact that different space harmonic components do not interact[13].

The total stator flux vector $\mathbf{\Lambda}_s$ can be separated into a part due to the stator currents and one due to the mutual coupling with the rotor circuit. For clarity of explanation each term will be developed separately.

A. Stator flux due to stator currents

For sinusoidally distributed windings the stator flux due to the stator currents $\mathbf{\Lambda}_{ss}$ is known to be [1]

$$\begin{bmatrix}\lambda_{ass}\\ \lambda_{bss}\\ \lambda_{css}\end{bmatrix}=\begin{bmatrix}L_{ls}+L_{ms} & -\frac{L_{ms}}{2} & -\frac{L_{ms}}{2}\\ -\frac{L_{ms}}{2} & L_{ls}+L_{ms} & -\frac{L_{ms}}{2}\\ -\frac{L_{ms}}{2} & -\frac{L_{ms}}{2} & L_{ls}+L_{ms}\end{bmatrix}\mathbf{i}_s \qquad (1)$$

where L_{ls} and L_{ms} are the leakage and magnetizing inductances of the stator windings. Applying the three-phase

space vector definition to (1) yields

$$\underline{\lambda}_{ss} = \frac{2}{3}\left(\lambda_{ass} + \underline{a}\lambda_{bss} + \underline{a}^2\lambda_{css}\right) \tag{2}$$

where $\underline{a}$ is the complex number $e^{j(2\pi/3)}$ and $\underline{\lambda}_{ss}$ is the complex space vector, thus

$$\underline{\lambda}_{ss} = \left(L_{ls} + \frac{3}{2}L_{ms}\right)\underline{i}_s \tag{3}$$

where

$$\underline{i}_s = \frac{2}{3}\left(i_{as} + \underline{a}i_{bs} + \underline{a}^2 i_{cs}\right) \tag{4}$$

is the space vector representation of the stator current.

The magnetizing inductance, L_{ms}, for a winding having N_s turns per phase is given by [1]

$$L_{ms} = \frac{\mu_o l r}{g} N_s^2 \left(\frac{\pi}{4}\right) \tag{5}$$

where l is the stack length, r the mean air-gap radius and g the air-gap length.

B. Stator flux due to rotor currents

The rotor cage is normally modeled as n identical and equally spaced loops [4], [5], [9]. As shown in Fig. 1 each loop is formed by two adjacent rotor bars and the connecting portions of the end rings between them. Each loop is magnetically coupled to all the other loops (circuits) and to all three stator phases.

The stator flux linkage due to the rotor currents is

$$\mathbf{\Lambda}_{sr} = \begin{bmatrix}\lambda_{asr}\\ \lambda_{bsr}\\ \lambda_{csr}\end{bmatrix} = \begin{bmatrix}L_{a1} & L_{a2} & \cdots & L_{an}\\ L_{b1} & L_{b2} & \cdots & L_{bn}\\ L_{c1} & L_{c2} & \cdots & L_{cn}\end{bmatrix}\begin{bmatrix}i_{r1}\\ \vdots\\ i_{rn}\end{bmatrix} \tag{6}$$

where L_{xi} represents the mutual inductance between the stator phase x and the rotor loop i. Neglecting the MMF drop in the iron, these inductances are conveniently calculated by means of winding functions [8], [11]. According to this theory the mutual inductance between two arbitrary machine windings "i" and "j" is given by

$$L_{ij}(\theta) = \mu_o l r \int_0^{2\pi} g^{-1}(\varphi,\theta) N_i(\varphi,\theta) N_j(\varphi,\theta) d\varphi \tag{7}$$

where θ is the angular rotor position with respect to some arbitrary reference, φ is a particular point along the air-gap, $g^{-1}(\varphi,\theta)$ is the inverse air-gap function and $N(\varphi,\theta)$ is the winding function defined as the spatial distribution of MMF due to a unit current flowing in the winding. If the air-gap is assumed to be uniform and small compared to the rotor radius the inverse air-gap function becomes simply a constant g^{-1} and it can be taken out of the integral. In this case, to find the mutual inductance we only need to define the winding functions.

Consider the stator windings and rotor bar disposition shown in Fig. 2. Taking as a reference the magnetic axis of phase a the normalized stator winding function for this phase is [11]

$$N_a(\theta) = \frac{N_s}{2}\cos(\theta) \tag{8}$$

The normalized winding functions of phases b and c are simply displaced by $\pm 120°$ with respect to N_a.

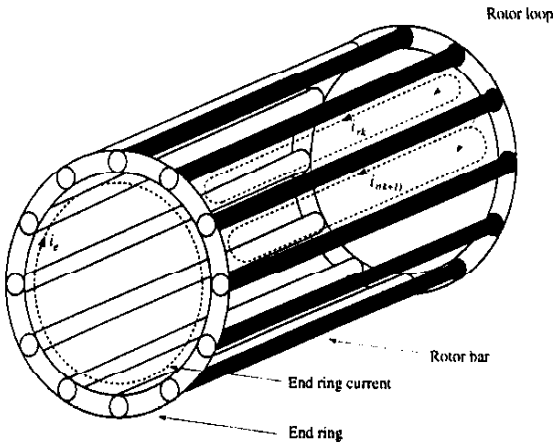

Fig. 1. Elementary rotor loops and current definitions.

The normalized winding function for the *i_th* rotor loop, given by the MMF distribution produced by one ampere of current flowing through the *i_th* loop, is shown in Fig. 2. For all the other loops the normalized winding functions are similar, changing only the relative phase angle as defined by the position of each loop with respect to the reference point. Mathematically, this function is defined by

$$N_i(\theta) = \begin{cases} -\alpha_r/2\pi & 0 < \theta \le \theta_i \\ 1 - \alpha_r/2\pi & \theta_i < \theta \le \theta_{i+1} \\ -\alpha_r/2\pi & \theta_{i+1} < \theta \le 2\pi \end{cases} \tag{9}$$

where α_r is the angle between two adjacent rotor bars and θ_i and θ_{i+1} define the position of the bars forming the loop.

The mutual inductance between phase a and the *i_th* rotor loop is

$$\begin{aligned} L_{ai} &= \frac{\mu_o l r}{g}\int_0^{2\pi} N_a(\theta) N_i(\theta) d\theta \\ &= \frac{\mu_o l r}{g}\frac{N_s}{2}\left[\sin\alpha_r \cos\theta_i - (1-\cos\alpha_r)\sin\theta_i\right] \end{aligned} \tag{10}$$

Since each rotor loop is symmetrically located along the rotor periphery, θ_i can be expressed in terms of an arbitrary rotor angle, θ_r, and the angle between adjacent rotor bars, α_r, as

$$\theta_i = \theta_r + (i-1)\alpha_r \tag{11}$$

By using trigonometric identities (10) can be written as

$$L_{ai}(\theta_i) = L_m \cos\left(\theta_r + (i-1)\alpha_r + \delta\right) \tag{12}$$

where

$$L_m = \frac{4}{\pi}\frac{\sin(\delta)}{N_s} L_{ms} \tag{13}$$

and

$$\delta = \frac{\alpha_r}{2} \tag{14}$$

The mutual inductance of the *i_th* rotor loop with respect to phases b and c are found by phase shifting L_{ai} by $\pm 120°$.

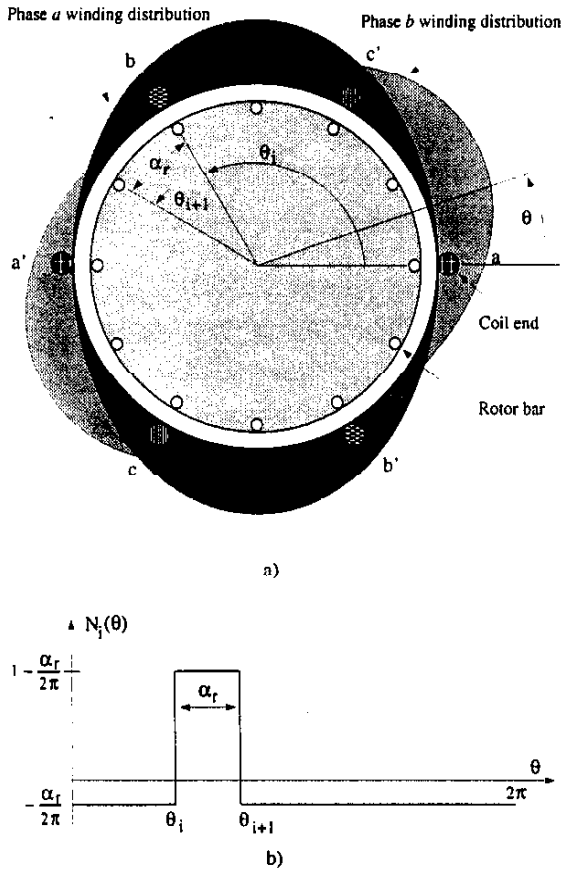

Fig. 2. a) Stator windings distribution; b) rotor loop winding function.

Using the Euler relation and substituting the mutual inductance expressions into (6) yields

$$\begin{bmatrix} \lambda_{asr} \\ \underline{a}\,\lambda_{bsr} \\ \underline{a}^2\lambda_{csr} \end{bmatrix} = \frac{L_m}{2}\left\{ e^{-j(\theta_r+\delta)} \begin{bmatrix} 1 & \underline{b}^{-1} & \cdots & \underline{b}^{1-n} \\ \underline{a} & \underline{a}\,\underline{b}^{-1} & \cdots & \underline{a}\,\underline{b}^{1-n} \\ \underline{a}^2 & \underline{a}^2\underline{b}^{-1} & \cdots & \underline{a}^2\underline{b}^{1-n} \end{bmatrix} + e^{j(\theta_r+\delta)} \begin{bmatrix} 1 & \underline{b} & \cdots & \underline{b}^{n-1} \\ 1 & \underline{b} & \cdots & \underline{b}^{n-1} \\ 1 & \underline{b} & \cdots & \underline{b}^{n-1} \end{bmatrix} \right\} \begin{bmatrix} i_{r1} \\ \vdots \\ i_{rn} \end{bmatrix} \tag{15}$$

where $\underline{b}$ is the complex number $e^{j\alpha_r}$. The mutual stator-rotor flux linkage complex vector $\underline{\lambda}_{sr}$ is obtained by adding all three rows of (15) and multiplying by 2/3, thus

$$\underline{\lambda}_{sr} = L_m \left\{ \left(1+\underline{a}+\underline{a}^2\right) e^{-j(\theta_r+\delta)} \left[1\,\underline{b}^{-1}\cdots\underline{b}^{1-n}\right] + e^{j(\theta_r+\delta)} \left[1\,\underline{b}\cdots\underline{b}^{n-1}\right] \right\} \begin{bmatrix} i_{r1} \\ i_{r2} \\ \vdots \\ i_{rn} \end{bmatrix} \tag{16}$$

Since $1+\underline{a}+\underline{a}^2 = 0$ the first term on the right hand side of (16) is always zero, therefore $\underline{\lambda}_{sr}$ simply becomes

$$\underline{\lambda}_{sr} = \frac{n}{2} L_m e^{j(\theta_r+\delta)} \underline{i}_r \tag{17}$$

where

$$\underline{i}_r = \frac{2}{n}\left[1\,\underline{b}\cdots\underline{b}^{n-1}\right] \begin{bmatrix} i_{r1} \\ i_{r2} \\ \vdots \\ i_{rn} \end{bmatrix} \tag{18}$$

defines the space vector representation of the rotor currents.

The total stator flux, given by the sum of (3) and (17), is

$$\underline{\lambda}_s = \underline{\lambda}_{ss} + \underline{\lambda}_{sr} = L_s \underline{i}_s + \frac{n}{2} L_m e^{j(\theta_r+\delta)} \underline{i}_r \tag{19}$$

where $L_s = L_{ls} + \frac{3}{2}L_{ms}$. Note that in this derivation no assumption has been made regarding the waveform of the rotor currents and (19) is valid for any type of excitation as well as during transient operation.

In space vector notation, the stator voltage $\underline{v}_s$ is known to be [1]

$$\underline{v}_s = r_s \underline{i}_s + p\underline{\lambda}_s \tag{20}$$

where r_s is the stator resistance. Taking the time derivative of (19) and substituting into (20) yields

$$\underline{v}_s = r_s \underline{i}_s + L_s p\underline{i}_s + \frac{n}{2} L_m e^{j(\theta_r+\delta)} \left(p + j\omega_r\right) \underline{i}_r \tag{21}$$

This expression has the same structure as the well known dq model available in the literature. The main difference being the phase angle introduced by the complex exponential term, which is due to the arbitrary choice of reference for the magnetic axis of the first rotor loop. Also, since a nonsinusoidal rotor bar distribution is considered the number of rotor bars appears explicitly.

III. Rotor Model

Given the structural symmetry of the rotor it is convenient to model the cage as n identical magnetically coupled circuits. One particular advantage of this approach is that it is applicable to rotors with non-integral number of bars per pole. For simplicity each loop is defined by two adjacent rotor bars and the connecting portions of the end rings between them.

For purpose of analysis each rotor bar and segment of end-ring is substituted by an equivalent circuit representing the resistive and inductive nature of the cage [4], [5], [12]. It is also convenient to carry out the analysis using mesh currents as the independent variables. Such an equivalent circuit is shown in Fig. 3.

In general there are $n+1$ independent meshes defined by the n rotor loops plus one formed by any one of the end rings. However, in the absence of an axial flux component the circumferential current in the end ring, i_e, is identically zero, hence it will not be considered here.

The loop equation for the k_th rotor circuit is

$$0 = 2\left(R_b + R_e\right) i_{rk} - R_b i_{r(k-1)} - R_b i_{r(k+1)} + p\lambda_{rk} \tag{22}$$

where R_b represents the bar resistance, R_e is the end-ring segment resistance, λ_{rk} is the total flux linked by the k_th loop and i_{rk} is the loop current. Since each loop is assumed to be identical (22) is valid for every loop, therefore the rotor voltage equation in matrix form is

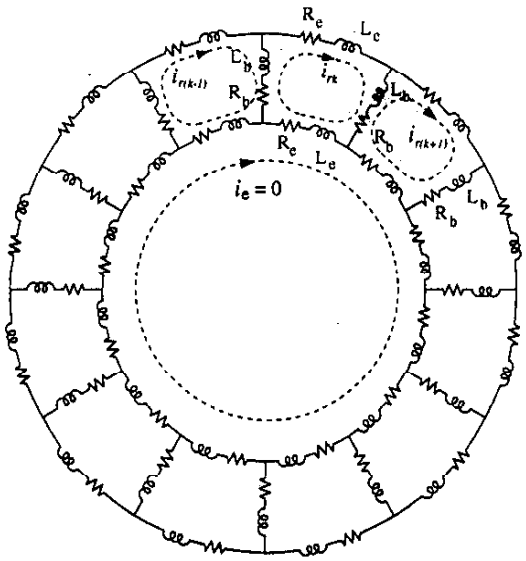

Fig. 3. Rotor cage equivalent circuit.

$$\begin{bmatrix}0\\0\\\vdots\\0\end{bmatrix}=\begin{bmatrix}R_o & -R_b & \cdots & -R_b\\ -R_b & R_o & \cdots & 0\\ \vdots & \vdots & \ddots & \vdots\\ -R_b & 0 & \cdots & R_o\end{bmatrix}\begin{bmatrix}i_{r1}\\i_{r2}\\\vdots\\i_{rn}\end{bmatrix}+p\begin{bmatrix}\lambda_{r1}\\\lambda_{r2}\\\vdots\\\lambda_{rn}\end{bmatrix} \tag{23}$$

with $R_o = 2\,(R_b + R_e)$.

The rotor equation in space vector form is obtained by applying the transformation given in (18) to (23) yielding

$$\underline{0} = r_r \underline{i}_r + p\underline{\lambda}_r \tag{24}$$

where $\underline{0}$ represents the zero voltage vector due to the squirrel cage and r_r is the equivalent rotor resistance in the subspace defined by the space vector transformation.

The total rotor flux, $\mathbf{\Lambda}_r = [\lambda_{r1}\ \lambda_{r2}\ \cdots\ \lambda_{rn}]^T$, can be divided into two components one due to the stator currents, $\mathbf{\Lambda}_{rs}$ and one due to the rotor currents, $\mathbf{\Lambda}_{rr}$. Again, for clarity of explanation, each component will be developed separately.

A. Rotor flux due to stator currents

The mutual coupling between rotor and stator, is given by

$$\mathbf{\Lambda}_{rs} = \begin{bmatrix}\lambda_{r1s}\\\lambda_{r2s}\\\vdots\\\lambda_{rns}\end{bmatrix} = \begin{bmatrix}L_{1a} & L_{1b} & L_{1c}\\ L_{2a} & L_{2b} & L_{2c}\\ \vdots & \vdots & \vdots\\ L_{na} & L_{nb} & L_{nc}\end{bmatrix}\begin{bmatrix}i_{as}\\i_{bs}\\i_{cs}\end{bmatrix} \tag{25}$$

Because of energy considerations, $L_{ix} = L_{xi}$ for $i = 1,\cdots,n$ and for $x = a,b,c$; and they correspond to those defined in II-B. Using complex notation and multiplying the rows of (25) by $1,\ \underline{b},\cdots,\underline{b}^{n-1}$ yields

$$\begin{bmatrix}\lambda_{r1s}\\\underline{b}\lambda_{r2s}\\\vdots\\\underline{b}^{n-1}\lambda_{rns}\end{bmatrix} = \frac{L_m}{2}\left\{ e^{-j(\theta_r+\delta)}\begin{bmatrix}1 & \underline{a} & \underline{a}^2\\ 1 & \underline{a} & \underline{a}^2\\ \vdots & \vdots & \vdots\\ 1 & \underline{a} & \underline{a}^2\end{bmatrix}\right.$$
$$\left. + e^{j(\theta_r+\delta)}\begin{bmatrix}1 & \underline{a}^2 & \underline{a}\\ \underline{b}^2 & \underline{a}^2\underline{b}^2 & \underline{a}\,\underline{b}^2\\ \vdots & \vdots & \vdots\\ \underline{b}^{2(n-1)} & \underline{a}^2\underline{b}^{2(n-1)} & \underline{a}\,\underline{b}^{2(n-1)}\end{bmatrix}\right\}\begin{bmatrix}i_{as}\\i_{bs}\\i_{cs}\end{bmatrix} \tag{26}$$

The complex vector $\underline{\lambda}_{rs}$, is obtained by adding all the rows of (26) and multiplying by $2/n$, thus

$$\underline{\lambda}_{rs} = \frac{L_m}{n}\left\{ n e^{-j(\theta_r+\delta)}\left[1\ \underline{a}\ \underline{a}^2\right]\right.$$
$$\left. + e^{j(\theta_r+\delta)}\left(1+\cdots+\underline{b}^{2(n-1)}\right)\left[1\ \underline{a}^2\ \underline{a}\right]\right\}\begin{bmatrix}i_{as}\\i_{bs}\\i_{cs}\end{bmatrix} \tag{27}$$

Since $1+\underline{b}^2+\cdots+\underline{b}^{2(n-1)} = 0$ and using the the definition of the stator current space vector $\underline{i}_s$, (27) reduces to

$$\underline{\lambda}_{rs} = \frac{3}{2}L_m e^{-j(\theta_r+\delta)}\underline{i}_s \tag{28}$$

B. Rotor flux due to rotor currents

The total flux linked by the *k_th* rotor circuit and due only to the rotor currents is given by

$$\lambda_{rkr} = L_{k1}i_{r1} + \cdots + L_{kn}i_{rn} + 2\,(L_e + L_b)\,i_{rk} - L_b\left(i_{r(k-1)} + i_{r(k+1)}\right) \tag{29}$$

where L_{ki} represents the mutual magnetic coupling between rotor loops k and i and L_{kk} is the self inductance of the *k_th* loop.

Because of the structural symmetry of the rotor (29) is valid for every loop, hence $\mathbf{\Lambda}_{rr}$ can be written in matrix form as

$$\begin{bmatrix}\lambda_{r1r}\\\lambda_{r2r}\\\vdots\\\lambda_{rnr}\end{bmatrix}=\begin{bmatrix}L_{11}+L_o & L_{12}-L_b & \cdots & L_{1n}-L_b\\ L_{21}-L_b & L_{22}+L_o & \cdots & L_{2n}\\ \vdots & \vdots & \ddots & \vdots\\ L_{n1}-L_b & L_{n2} & \cdots & L_{nn}+L_o\end{bmatrix}\begin{bmatrix}i_{r1}\\i_{r2}\\\vdots\\i_{rn}\end{bmatrix} \tag{30}$$

with $L_o = 2(L_b + L_e)$. The self and mutual inductances defined in (30) are obtained by means of the winding functions. The self inductance of the *k_th* loop is found to be [6]

$$L_{kk} = \frac{\mu_o l r}{g}\int_0^{2\pi} N_k^2(\theta)d\theta = \frac{\mu_o l r}{g}\alpha_r\left(1-\frac{\alpha_r}{2\pi}\right) \tag{31}$$

and the mutual inductance between the *k_th* and the *i_th* rotor loops is

$$L_{ki} = \frac{\mu_o l r}{g}\int_0^{2\pi} N_k(\theta)N_i(\theta)d\theta = \frac{\mu_o l r}{g}\left(-\frac{\alpha_r^2}{2\pi}\right) \tag{32}$$

As expected both L_{kk} and L_{ki} are constants that only depend on the rotor dimensions and not on their relative position. Substituting (31) and (32) into (30) and multiplying each row by $1,\ b,\cdots,b^{n-1}$ yields

$$\begin{bmatrix} \lambda_{r1r} \\ \underline{b}\lambda_{r2r} \\ \vdots \\ \underline{b}^{n-1}\lambda_{rnr} \end{bmatrix} = \begin{bmatrix} L_{kk}+L_o & \underline{b}^{n-1}(L_{kl}-L_b) & \cdots & \underline{b}(L_{kl}-L_b) \\ \underline{b}(L_{kl}-L_b) & L_{kk}+L_o & \cdots & \underline{b}^2 L_{kl} \\ \vdots & \vdots & \ddots & \vdots \\ \underline{b}^{n-1}(L_{kl}-L_b) & \underline{b}^{n-2}L_{kl} & \cdots & L_{kk}+L_o \end{bmatrix} \begin{bmatrix} i_{r1} \\ \underline{b}i_{r2} \\ \vdots \\ \underline{b}^{n-1}i_{rn} \end{bmatrix} \tag{33}$$

where we have used the identity $\underline{b}^{n+m} = \underline{b}^m$.

Adding all the rows in (33) and reducing terms we obtain the rotor flux complex vector due to the rotor currents

$$\begin{aligned} \underline{\lambda}_{rr} &= \left(L_o + \frac{n}{n-1} L_{kk} - 2L_b \cos\alpha_r \right) \underline{i}_r \\ &= \underbrace{\left(2L_b(1-\cos\alpha_r) + 2L_e + \frac{\mu_o l r}{g}\alpha_r \right)}_{L_r} \underline{i}_r \end{aligned} \tag{34}$$

The proportionality constant L_r corresponds to the equivalent rotor inductance. Note that its value is expressed only in terms of rotor dimensions and bar and end-ring inductance values.

The total rotor flux vector, defined as the sum of (28) and (34), is

$$\underline{\lambda}_r = \frac{3}{2} L_m e^{-j(\theta_r+\delta)} \underline{i}_s + L_r \underline{i}_r \tag{35}$$

C. Rotor equivalent resistance

The equivalent rotor resistance is obtained from the first term on the right-hand-side of (23). The procedure is identical to the one used to obtain the rotor flux therefore it will not be repeated here. It suffices to say that after multiplying each row of the first term in (23) by $1, \underline{b}, \cdots, \underline{b}^{n-1}$, adding and simplifying it yields

$$\begin{aligned} r_r &= R_o - R_b \left(\underline{b}^{n-1} + \underline{b} \right) \\ &= 2R_e + R_b + 2R_b (1 - \cos\alpha_r) \end{aligned} \tag{36}$$

Note that equivalent rotor resistance r_r is expressed in terms of the actual bar and end ring resistance values making it straight forward to include changes in their values due to temperature or skin effect.

Finally, substituting (35) into (24) yields the rotor equation in the subspace defined by the rotor space vector transformation

$$\underline{0} = r_r \underline{i}_r + \frac{3}{2} L_m e^{-j(\theta_r+\delta)} (p - j\omega_r) \underline{i}_s + L_r p \underline{i}_r \tag{37}$$

Equations (21) and (37) correspond to the complex vector model of the squirrel cage induction machine and fully define the electrical behavior for both steady state and transient operation.

IV. Complex Vector Equivalent Circuit

It is known that the sinusoidal coupling between the stator and rotor circuits can be eliminated by referring all the equations to a common reference frame [14]. Figure 4 shows an arbitrary dq reference frame rotating at angular speed ω. The required dq variables in this common reference frame are defined by the vector transformations

$$\begin{aligned} \underline{i}_{qds} &= \tfrac{2}{3} e^{-j\theta} \underline{i}_s \\ \underline{i}_{qdr} &= \tfrac{2}{3} \sqrt{\tfrac{n}{3}} e^{-j(\theta-\theta_r-\delta)} \underline{i}_r \end{aligned} \tag{38}$$

Applying this transformation to (21) and (37) yields

$$\underline{v}_{qds} = r_s \underline{i}_{qds} + L_s p \underline{i}_{qds} + \frac{3}{2}\sqrt{\frac{n}{3}} L_m p \underline{i}_{qdr} + j\omega \underline{\lambda}_{qds} \tag{39}$$

$$\underline{0} = r_r \underline{i}_{qdr} + L_r p \underline{i}_{qdr} + \frac{3}{2}\sqrt{\frac{n}{3}} L_m p \underline{i}_{qds} + j(\omega - \omega_r) \underline{\lambda}_{qdr} \tag{40}$$

where

$$\underline{\lambda}_{qds} = L_s \underline{i}_{qds} + \frac{3}{2}\sqrt{\frac{n}{3}} L_m \underline{i}_{qdr} \tag{41}$$

$$\underline{\lambda}_{qdr} = \frac{3}{2}\sqrt{\frac{n}{3}} L_m \underline{i}_{qds} + L_r \underline{i}_{qdr} \tag{42}$$

The corresponding equivalent circuit representing the machine in an arbitrary rotating reference frame is shown in Fig. 4.

The analysis carried out so far has implicitly assumed a machine having only one pair of poles, the extension to multi-pole structures is quite straight forward and it only requires one to substitute mechanical angles by their electrical equivalents.

It is important to point out that in contrast to the usual full set of differential equations required to solve for rotor bar currents the use of the space vector transformation defined in (18) gives a much simpler description of the machine, regardless of the number of rotor bars, thus providing a faster analysis tool.

V. Inverse Current Transformation

In general the n rotor currents need to be mapped into a full n-dimensional vector space. This new n-dimensional space is defined by the transformation [16]:

$$\begin{bmatrix} \underline{i}_r^0 \\ \underline{i}_r^1 \\ \vdots \\ \underline{i}_r^{n-1} \end{bmatrix} = \begin{bmatrix} 1 & 1 & \cdots & 1 \\ 1 & \underline{b} & \cdots & \underline{b}^{n-1} \\ \vdots & \vdots & \ddots & \vdots \\ 1 & \underline{b}^{n-1} & \cdots & \underline{b}^{(n-1)(n-1)} \end{bmatrix} \begin{bmatrix} i_{r1} \\ i_{r2} \\ \vdots \\ i_{rn} \end{bmatrix} \tag{43}$$

where $\underline{i}_r^i$ represents the i_th rotor current in the new space.

Upon applying (43) to the equations of a symmetrical squirrel cage machine it can be shown [15] that the transformed rotor variables, due to lack of excitation, are all identically zero except $\underline{i}_r^1$ and $\underline{i}_r^{n-1}$. Therefore only the second and last column of the inverse transformation matrix are of interest. Furthermore, from (43) it is clear that $\underline{i}_r^1$ corresponds to the space vector definition given in (18) and $\underline{i}_r^{n-1}$ is the complex conjugate. Hence, taking the inverse transformation and substituting yields

$$\begin{bmatrix} i_{r1} \\ i_{r2} \\ i_{r3} \\ \vdots \\ i_{rn} \end{bmatrix} = \frac{1}{n} \begin{bmatrix} 1 & 1 \\ \underline{b}^{-1} & \underline{b}^{1-n} \\ \underline{b}^{-2} & \underline{b}^{2(1-n)} \\ \vdots & \vdots \\ \underline{b}^{1-n} & \underline{b}^{-(1-n)^2} \end{bmatrix} \begin{bmatrix} \underline{i}_r \\ \underline{i}_r^* \end{bmatrix} \tag{44}$$

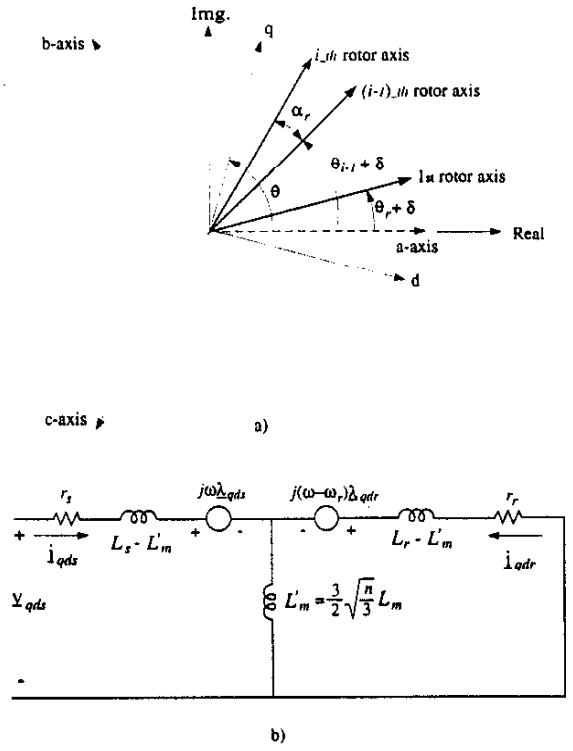

Fig. 4. a) Common reference frame definition; b) Complex vector equivalent circuit.

where the superscript * denotes complex conjugate. Eq. (44) shows that, for a symmetrical squirrel cage machine, only the complex conjugate subspaces are externally excited through the stator coupling while the rest can never be excited. Therefore the original n-dimensional space can be fully represented by the bi-dimensional subspace spanned by (18). Finally the inverse transformation is simply

$$\begin{aligned} i_{ri} &= \frac{2}{n} Re\left\{\underline{b}^{-(i-1)}\underline{i}_r\right\} \\ &= \frac{2}{n}\left[i_{xr}\cos(i-1)\alpha_r + i_{yr}\sin(i-1)\alpha_r\right] \end{aligned} \tag{45}$$

where Re represents the real part and i_{xr} and i_{yr} are the real and imaginary components of the complex vector $\underline{i}_r$. Note that this result is completely general and it does not assume any symmetry in the rotor current distribution.

VI. Electromagnetic Torque

Neglecting saturation the electromagnetic torque can be expressed as the partial variation of the co-energy with respect to rotor position [1], [6]:

$$T_e = \mathbf{i}_s^T \frac{\partial \mathbf{L}_{sr}}{\partial \theta_r}\,\mathbf{i}_r \tag{46}$$

where $\mathbf{i}_r = [i_{r1}\; i_{r2}\cdots i_{rn}]^T$ and $\mathbf{L}_{sr}$ corresponds to the rotor-stator mutual inductance matrix. After some matrix manipulation the mutual inductance can be written as

$$\begin{aligned} \mathbf{L}_{sr} = \frac{L_m}{2}\Big\{ & e^{j(\theta_r+\delta)}\begin{bmatrix}1\\ \underline{a}^2\\ \underline{a}\end{bmatrix}\left[1\;\underline{b}\cdots\underline{b}^{n-1}\right] \\ & + e^{-j(\theta_r+\delta)}\begin{bmatrix}1\\ \underline{a}\\ \underline{a}^2\end{bmatrix}\left[1\;\underline{b}^{-1}\cdots\underline{b}^{1-n}\right]\Big\} \end{aligned} \tag{47}$$

Note that only the exponential terms depend on the rotor position, hence the partial differentiation is quite easily obtained. After differentiating and pre-multiplying by $\mathbf{i}_s^T$ and post-multiplying by $\mathbf{i}_r$ yields

$$T_e = -\left(\frac{3}{2}\right)\left(\frac{n}{2}\right) L_m Im\left\{e^{j(\theta_r+\delta)}\,\underline{i}_s^*\,\underline{i}_r\right\} \tag{48}$$

where Im represents the imaginary part.

It is important to point out that (48) is similar to the usual expression derived for wound rotor machines. The term $n/2$ arises from the arbitrary constant in the definition of the rotor current space vector and the inductance term L_m includes the equivalent of the turns ratio found in the usual model.

VII. Simulation Results

To validate the proposed complex vector model a set of simulations was prepared. The main objective of the simulations is to compare the results of the proposed model to those of the full matrix model of the induction machine. The full matrix model has been well documented in the literature and its correctness has been proven over the years. The most recent examples can be found in [9], [12]. For simulation purposes a typical 5 HP, 4 pole machine was used. The results from the full matrix model and the complex vector model are shown superimposed in figures 5 and 6 for sinusoidal excitation. Fig. 7 shows the results for nonsinusoidal excitation. The agreement in all cases is perfect. The computation times required in each case are shown in Table I . The reduction in computational time achieved by the complex vector model is overwhelming. Note that both models fully predict the rotor bar and end-ring currents. However, at high speeds the full matrix model is prone to larger numerical errors due to the multiple matrix inversions combined to the rapid change in mutual inductance. Decreasing the integration step helps minimize this error, however this increases the computation time even more. The complex vector model, on the other hand, is free of such problems.

VIII. Three-phase Equivalent Parameters

Another important advantage of the complex vector model is its ability to predict the parameters of an equivalent wound rotor machine. The equivalent parameters are most easily obtained by introducing a slight modification to the rotor current space vector definition

$$\underline{i}'_r = \frac{n}{3}\frac{L_m}{L_{ms}} e^{j\delta}\underline{i}_r \tag{49}$$

Substituting $\underline{i}'_r$ into equations (21) and (37) and comparing to the equations of a sinusoidally wound rotor induc-

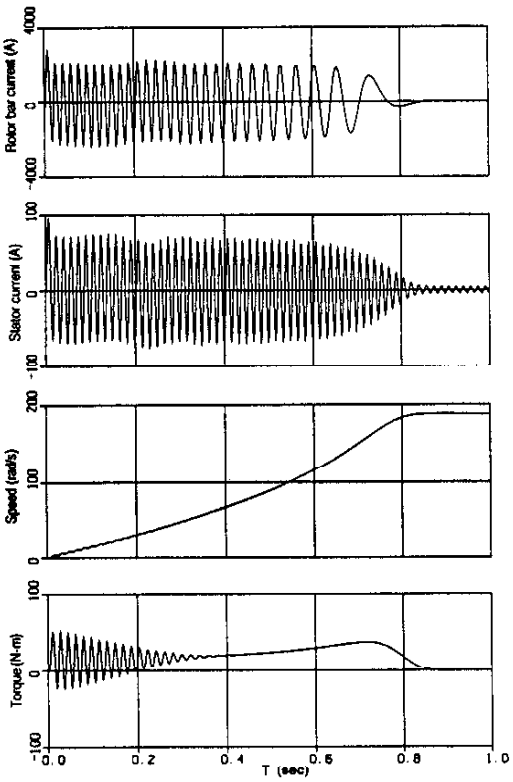

Fig. 5. Complex vector and full matrix model results (superimposed). Rotor bar current, stator current, rotor speed and electromagnetic torque during free acceleration.

tion machine leads to the equivalent stator referred rotor resistance

$$r'_r = \left(\frac{3\pi^2}{8}\right)\frac{N_s^2}{n\sin^2\delta}\left[R_b\left(1-\cos\alpha_r\right)+R_e\right] \qquad (50)$$

and the equivalent rotor leakage inductance

$$L'_{lr} = \frac{6}{n}\left(\frac{\pi}{4}\right)^2 N_s^2\left[2L_b+\frac{L_e}{\sin^2\delta}\right]+\frac{3}{2}L_{ms}\left[\frac{\delta^2}{\sin^2\delta}-1\right] \qquad (51)$$

Alternate forms to obtain the equivalent rotor parameters of a squirrel cage machine are presented in [2], [4]. The technique used is based on harmonic analysis and to obtain a closed form solution for the rotor leakage flux some approximations need to be made. Specifically, some of the spatial harmonic components produced by the rotor fundamental time harmonic component are neglected. This yields an approximate value of equivalent leakage inductance given by

$$L'_{lr} \approx \frac{6}{n}\left(\frac{\pi}{4}\right)^2 N_s^2\left[2L_b+\frac{L_e}{\sin^2\delta}\right]+\frac{3}{4}L_{ms}\left[\frac{\delta^2}{\sin^2\delta}-1\right] \qquad (52)$$

On the other hand the complex vector model is based on winding functions which take into account all the harmonic components at once. Also, the novel expression for the leakage inductance derived here has the virtue of simplicity without using the concepts of differential and zig-zag leakages.

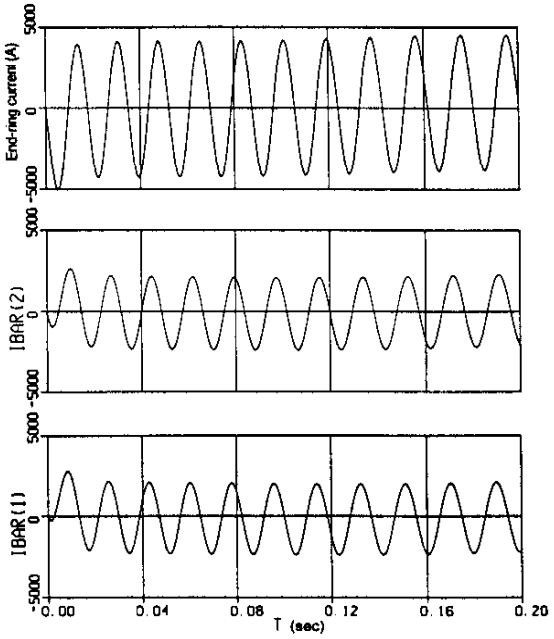

Fig. 6. Complex vector and full matrix model results (superimposed). Rotor currents in two adjacent rotor bars and in the segment of end-ring between them during the initial transient.

The difference between the exact value of L'_{lr} (51) and the approximate one (52) is the coefficient of the last term with the exact expression being twice as large. The relative importance of the error depends on the expression between the square brackets. When the number of rotor bars is large $\delta \to 0$ and the error is small. Conversely for rotor with fewer bars the error may be significant. As an example, the computations for rotors having 24 and 48 bars are presented in Table II.

The effect of using the approximate value of leakage inductance on the torque and speed curves for the 5 HP machine used in the simulation is shown in Fig. 8. In this figure the dotted line corresponds to the results of the dq model with L'_{lr} computed using (52) while the solid line corresponds to the superimposed solutions of the full matrix model, the complex vector model and the dq model with L_{lr} computed using (51).

TABLE I
REAL TIME REQUIRED TO RUN SIMULATIONS

Simulated time	Computation time	
	Full Matrix	Complex Vector
1 sec	498 sec	3 sec

TABLE II
LEAKAGE INDUCTANCE CALCULATIONS

24 bars		48 bars	
Ref. [2]	Comp. vector	Ref. [2]	Comp. vector
2.824 mH	4.000 mH	2.510 mH	2.801 mH

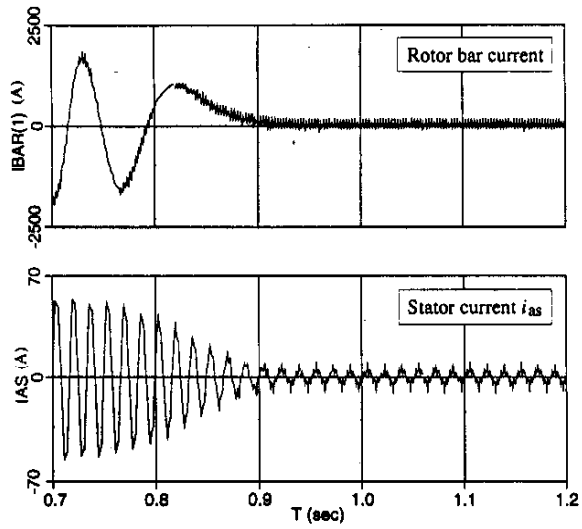

Fig. 7. Complex vector and full matrix model results (superimposed). Stator and rotor bar currents for nonsinusoidal excitation (six-step).

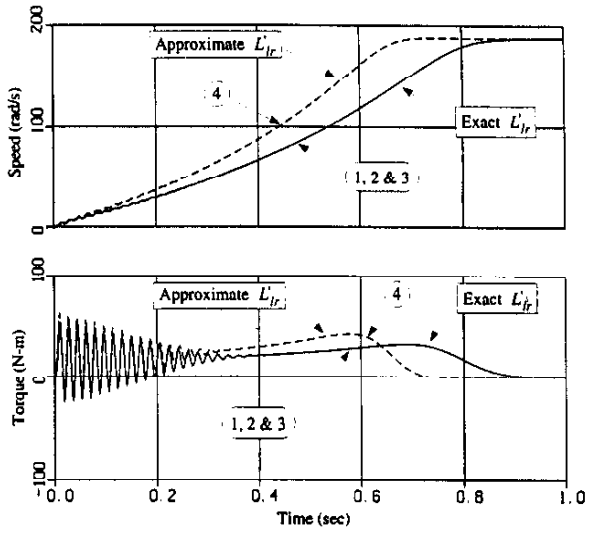

Fig. 8. Change in machine dynamics with rotor leakage inductance (24 rotor bars). 1) full matrix model, 2) space vector model, 3) dq model using equivalent parameters derived from space vector model, 4) dq model using equivalent parameters derived from traditional harmonic analysis [2].

IX. Conclusions

A detailed mathematical model of a squirrel cage induction machine has been developed. It has been shown that the use of complex space vectors leads to a simple d-q model without giving up any information regarding the actual rotor bar and end-ring currents. Note that this is true during both transient and steady state behavior and it does not assume sinusoidal currents.

The number of equations needed to fully represent the machine is independent of the number of rotor bars considered and the resulting equations have a similar structure to the one found in the usual d-q model. Because of the minimum number of equations used in the final model the computation time required to simulate the machine is drastically reduced. The three-phase equivalent rotor parameters in terms of actual rotor bar and end-ring resistance and inductance values are also obtained.

REFERENCES

[1] D. W. Novotny and T. A. Lipo, *Vector Control and Dynamics of AC Drives*, Clarendon Press-Oxford, 1996.

[2] A. S. Langsdorf, *Theory of Alternating Current Machinery*, Second Edition, McGraw-Hill, 1955.

[3] P. L. Alger, *Induction Machines*, Gordon and Breach Science Publishers, Second Edition, 1970.

[4] T. A. Lipo, *Introduction to AC Machine Design*, University of Wisconsin-WisPERC, 1996.

[5] A. K. Wallace and A. Wright, *"Novel simulation of cage windings based on mesh circuit model"*, IEEE Transactions on Power App. and Systems, Vol. PAS-93, No. 1, January/February 1974, pp. 377-382.

[6] H. A. Toliyat, *"Analysis of concentrated winding induction and reluctance machines for adjustable speed drive applications"*, Ph.D. Dissertation, University of Wisconsin-Madison, 1991.

[7] H. R. Fudeh and C. M. Ong, *"Modeling and analysis of induction machines containing space harmonics"*, Parts 1, 2, and 3, IEEE Transactions on Power App. and Systems, Vol. PAS-102, No. 8, August 1983, pp. 2608-2628.

[8] T. A. Lipo, *Theory and Control of Synchronous Machines*, ECE 511 Class Notes, ECE Department, University of Wisconsin-Madison, 1991.

[9] X. Luo, Y. Liao, H. A. Toliyat, A. El-Antably, and T. A. Lipo, *"Multiple couple circuit modeling of induction machines"*, IEEE Transactions on Industry Applications, Vol. 31, No. 2, March/April 1995, pp. 311-317.

[10] A. K. Wallace, R. Spée, and H. K. Lauw, *"Dynamic modeling of brushless doubly-fed machines"*, IEEE Industry Applications Society 1989 Annual Meeting, San Diego California, 1989, pp. 329-334.

[11] N. L. Schmitz and D. W. Novotny, *Introductory Electromechanics*, Ronald Press, New York, 1965.

[12] H. A. Toliyat and T. A. Lipo, *"Transient analysis of cage induction machines under stator, rotor bar, and end ring faults"*, IEEE Transactions on Energy Conversion, Vol. 10, No. 2, June 1995, pp. 241-247.

[13] S. A. Nasar, *"Electromechanical energy conversion in nm-winding double cylindrical structures in presence of space harmonics"*, IEEE Transactions on Power App. and Systems, Vol. PAS-87, No. 4, April 1968, pp. 1099-1106.

[14] P. Krause and C. Thomas, *"Simulation of symmetrical induction machinery"*, IEEE Transactions on Power App. and Systems, Vol. PAS-84, No. 11, Nov 1965, pp. 1038-1053.

[15] A. Muñoz-García, *"Analysis and control of a dual stator winding squirrel cage induction machine for high performance drives"*, Preliminary Ph.D. Thesis proposal, University of Wisconsin-Madison, 1997.

[16] D. C. White and H. H. Woodson, *Electromechanical Energy Conversion*, New York, John Wiley & Sons, 1959.